Journal of Theoretical Biology 611 (2025) 112191

Contents lists available at ScienceDirect

Journal of Theoretical Biology

journal homepage: www.elsevier.com/locate/jtbi

Revisiting a demographic model of pest infestation in farming

Giuseppe Buffoni [a,1], Sara Pasquali [a,*], Cinzia Soresina [b]

[a] CNR-IMATI "Enrico Magenes", via Alfonso Corti 12, 20133, Milano, Italy
[b] Dipartimento di Matematica, Università di Trento, via Sommarive 14, 38123, Povo, (TN), Italy

ARTICLE INFO

Keywords:
Stage-structured population
Diapause
Density-dependent fecundity
Pests

ABSTRACT

Reliable simulations of pest population dynamics are essential tools for effective pest management. Here we present a demographic model designed to describe overwintering stage-structured population dynamics. In addition to accounting for development, mortality, and fecundity, the model explicitly incorporates diapause, a key physiological process enabling pests to survive winter conditions. We detail the formulation of the mortality rate function based on the development rate and the proportion of individuals dying within each developmental stage. Simulations are performed for the case of *Lobesia botrana*, a major vineyard pest. Results show, under both constant and fluctuating temperature regimes, the necessity of employing a density-dependent fecundity function to regulate population growth. Under constant temperature conditions, when fecundity depends on total population density, the system dynamics converge to a steady state regardless of the temporal discretization step, though peak values vary. Conversely, if fecundity is a function of adult density only, the model yields periodic oscillations. Under variable temperature regimes, diapause facilitates seasonal population resurgence and mitigates peak pupal and adult densities in the fall.

1. Introduction

Pest management strategies are founded on a comprehensive understanding of pest phenology under varying environmental conditions that influence development, mortality, and fecundity, thereby driving fluctuations in population abundance. The capacity to accurately predict pest population dynamics under such variable conditions is instrumental for reducing pesticide interventions, enhancing product quality, and promoting the health and sustainability of agricultural production. Mathematical models serve as indispensable tools to describe and forecast insect population behavior.

The importance of mathematical models in integrated pest management has long been acknowledged. Getz and Gutierrez (1982) provided a historical review of systems analysis in crop protection, while Curry and Feldman (1987) compiled mathematical methodologies for modeling the population dynamics of poikilotherms. Mechanistic models driven primarily by environmental variables, especially temperature, are widely employed to characterize pest population dynamics (see references in Gilioli et al. (2016)). Since pests typically pose a threat at a specific life stage (Kumar and Rathor, 2020), it is essential to consider stage-structured populations (Kooi and Kelpin, 2003; Manly, 1990), wherein stages are demarcated by distinct biological events such as egg hatching, molting, adult emergence, and onset of oviposition. Key biological parameters characterize individual behavior at each stage, including stage-specific development times, fecundity profile as a function of female "age", and mortality rates. Accurate knowledge of these parameters is crucial for developing population dynamics models capable of realistically representing infestation growth over time (Kontopoulos et al., 2024). Stage-structured models can be classified as demographic or phenological (Pasquali et al., 2019). Demographic models describe population abundance as a function of time and age, whereas phenological models focus on the cumulative flux of individuals transitioning through stages.

Population dynamics models adopt either Lagrangian or Eulerian approaches (Buffoni and Pasquali, 2007). The Lagrangian formalism, often termed individual-based modeling (random flights, Monte Carlo methods), simulates the life histories of numerous individuals, subsequently aggregating results to infer population dynamics. However, this approach does not yield insights into population evolution prior to computation. Conversely, the Eulerian formalism employs balance equations: hyperbolic PDEs in the Von Foerster approach and parabolic PDEs in the Kolmogorov approach. The Von Foerster equations (Hoppenstaedt, 1975) treat development deterministically, while the Kolmogorov equations model development as a stochastic process (Buffoni and Pasquali, 2010, 2013; Pasquali, 2021; Pasquali and Trivellato, 2023).

* Corresponding author.
E-mail address: sara.pasquali@mi.imati.cnr.it (S. Pasquali).
[1] Giuseppe Buffoni passed away on December 5th, 2024.

https://doi.org/10.1016/j.jtbi.2025.112191
Received 27 August 2024; Received in revised form 4 June 2025; Accepted 9 June 2025
Available online 14 June 2025

This study focuses on the implementation of simple yet reliable Von Foerster demographic models for simulating pest infestation dynamics, particularly in agricultural contexts. By *simple*, we refer to limiting the number of stages through the introduction of macro-stages (Murdoch and Briggs, 1996), i.e., grouping biologically similar individual stages into single aggregated stages (for instance, combining multiple larval stages). This strategy serves to reduce the model's parameter complexity and facilitate analytical tractability, though it may also reflect limitations in available data. Furthermore, the dynamics of the structured population is assumed to be governed by the primary biological processes underpinning an individual's life history: development, reproduction, and mortality. Generally, the rates of these processes are functions of abiotic variables varying over time, chiefly temperature and feeding.

The model presented herein extends conventional demographic frameworks by explicitly incorporating the diapause process, which enables individuals to survive adverse winter conditions through halted development until favorable conditions return (Gill et al., 2017). Although recent studies have increasingly examined diapause (e.g., Ewing et al. (2021); Gutierrez et al. (2012); Lou et al. (2019); Pak et al. (2022)), it is still little explored. For instance, in Pak et al. (2022), where population dynamics are modeled via differential equations with distinct developmental rates for diapausing individuals, diapause induction depends solely on the day of the year. In contrast, our approach models diapause as a function of average temperature over a time interval and photoperiod. Moreover, unlike Sperandio et al. (2024), who model only diapause termination, our model accounts for both entry and exit conditions. Diapausing individuals form a distinct stage governed by their own dynamic equation, differing from Lou et al. (2019) where diapause effects are incorporated through modified dynamics within fixed stages over the diapause interval.

While laboratory data under constant temperature conditions are available for development durations in many species, mortality rate data are often lacking, complicating the estimation of mortality functions. Statistical approaches leveraging population dynamics data have been developed to estimate parameters in the absence of direct biological measurements (Gilioli et al., 2016; Lanzarone et al., 2017; Pasquali et al., 2022), it is also possible to estimate development and mortality rate functions concurrently (Rossini et al., 2022, 2023). Here, we propose a mathematical formulation of the mortality rate function derived from the development rate and the proportion of dying individuals. Additionally, to prevent uncontrolled population growth when mortality is insufficient, we introduce density dependence in fecundity rates, consistent with literature where density dependence is incorporated in both fecundity and mortality (Curry and Feldman, 1987; Lou and Sun, 2022; Mcnair, 1995).

The Von Foerster model is applied to the dynamics of the grape berry moth *Lobesia botrana*, a major vineyard pest in the Mediterranean basin (Cabi, 2014). The biodemographic functions of *L. botrana* have been estimated (Gilioli et al., 2016; Gutierrez et al., 2012). This study analyzes the impacts of density-dependent fecundity and diapause processes through two-year simulations.

The paper is structured as follows. Section 2 summarizes the Von Foerster demographic equations utilized. Section 3 formulates the rates of key biological processes under simplified population structures, revisiting and detailing the derivation of mortality rates from development rates and proportions of dying individuals. Section 4 integrates the diapause process within the Von Foerster framework. Section 5 describes the numerical discretization, emphasizing the handling of positive versus null development rates. Section 6 presents the case study, including biological annual cycle descriptions, refined dynamic equations with parameter estimates for *L. botrana*, and numerical simulation results illustrating system behaviour over one or more years. Finally, Section 7 offers concluding remarks. The simulation code is publicly accessible on GitHub (Buffoni et al., 2025).

2. The basic equations of the demographic model

Suppose the insect population is divided into s stages, with stages 1 to $s-1$ representing the immature individuals and stage s representing the reproductive adults. Denote by D^i the average degree-days necessary for the development of an individual in stage $i < s$, and D^s as the average life span of an adult. We are interested in the average number of individuals (expressed as either number of individuals per m^2 of soil or individuals per plant). We consider

$$\phi^i(t,x)\,dx \;=\; \text{average number of individuals in stage } i \text{ at time } t, \text{ with physiological age in } (x, x+dx).$$

Here, it is assumed that the "status" of an individual can be identified by its stage and a single physiological variable, representing its physiological age within the stage in terms of degree-days ($^\circ C\,d$) (Curry and Feldman, 1987). It will be denoted by x, and more precisely it represents the degree-days experienced by an individual in a stage, i.e. x (measured in $^\circ C\,d$) is the integral of the temperature $T(t)$ (measured in $^\circ C$) over time t (measured in d) between the initial time in the stage and the current time. From now on, x will simply be referred to as age.

From an Eulerian perspective, and within a deterministic framework, the dynamics is described here in terms of the Von Foerster hyperbolic equations (Hoppenstaedt, 1975) written as

$$\frac{\partial \phi^i}{\partial t} + v^i(t)\frac{\partial \phi^i}{\partial x} + m^i(t)\phi^i = S^i(t), \quad t > t_0,\ x \in (0, D^i), \tag{1}$$

$$\phi^i(t,0) = F^i(t), \tag{2}$$

$$\phi^i(t_0,x) = \hat{\phi}^i(x), \tag{3}$$

where $i = 1, 2, \ldots, s$, $v^i(t)$ (≥ 0) and $m^i(t)$ (> 0) are the specific developmental and mortality rates, respectively, assumed independent of age x, $S^i(t)$ (≥ 0) are possible external inputs to the system, and $\hat{\phi}^i(x)$ (≥ 0) is the initial distribution. The terms $F^i(t)$ in the boundary condition Eq. (2) represent the input of individuals into stage i at time t.

The function $F^1(t)$ describes egg production, assumed to be given by

$$F^1(t) = \sigma \int_0^{D^s} b(t,x)\,\rho\phi^s(t,x)\,dx, \tag{4}$$

where $b(t,x)$ is the specific fertility rate expressed as eggs/female/$^\circ C d$ (taking into account also temperature and diet effects). Note that if $\hat{b}(t,x)$ is the specific fertility rate expressed in terms of eggs/female/d, then

$$b(t,x) = \frac{\hat{b}(t,x)}{v^1(t)}.$$

Finally, ρ is the ratio

$$\rho = \frac{\text{females}}{\text{females} + \text{males}}$$

and the factor σ is a possible nonlinear function of the population, representing a basic feedback due to population size on the recruitment (Bergh and Getz, 1988).

Two different cases have been considered to compute the fluxes F^i: $v^i(t) > 0$ and $v^i(t) = 0$. When $v^i(t) > 0$, the terms $F^i(t)$, $i > 1$, are obtained by imposing the continuity of the fluxes of individuals from stage $i-1$ into stage i:

$$F^i(t) = \phi^{i-1}(t, D^{i-1})v^{i-1}(t)/v^i(t), \quad i > 1. \tag{5}$$

When $v^i(t) = 0$, Eq. (1) becomes an ODE, and the time evolution of $\phi^i(t,x)$ is only influenced by the mortality and possibly by the external input $S^i(t)$. Moreover, this situation gives rise to an accumulation of individuals in stage i at $x = 0$ at times t when $v^{i-1}(t) > 0$ and $v^i(t) = 0$. In Table 1 the values that should be assigned to $\phi^i(t,0)$ in the discrete equations, for all the possible outcomes, are reported.

Finally, the average number $\bar{N}^i(t)$ of individuals in stage i at time t, and the total population $N(t)$ are obtained by

$$\bar{N}^i(t) = \int_0^{D^i} \phi^i(t,x)dx \qquad N(t) = \sum_{i=1}^{s} \bar{N}^i(t).$$

For the sake of simplicity, we do not take into account dependence on the physiological age for development and mortality, even if the deterministic formulation Eqs. (1)–(3), with v^i and m^i dependent also on the age x, is widely proposed and studied in the literature (see, for instance, Abia et al. (2004); Angulo and Lopez-Marcos (2004); Buffoni and Pasquali (2007); Murphy (1983); Sulsky (1994)).

3. Rates of biological processes

The development, mortality, and fecundity rates of insect pests are strongly influenced by environmental conditions, among which temperature plays a major role (Kontopoulos et al., 2024; Pawar et al., 2024). The dependence of insect biology on climate change has been studied extensively for many years (Bhagarathi and Maharaj, 2023; Subedi et al., 2023). Thus, we assume that the rates of biological processes are time-dependent through temperature, but remain independent of the physiological age x of individuals within the stage.

3.1. Developmental rates

The development process of an individual in stage i is characterized by the following critical parameters:

- the minimum and maximum temperature thresholds T^i_{min} and T^i_{max} (assuming $T^i_{min} < T^i_{max}$) determining the temperature range that supports a positive development,
- the mean total requirement D^i of degree-day units to complete the process.

The developmental rate of an individual is defined as the ratio between the average age increment Δx gained during a time interval Δt. Two quantities can be defined to estimate the developmental rate of an individual:

$$\frac{\Delta x}{\Delta t} = V^i \text{ in } {}^\circ C, \quad \frac{\Delta x}{D^i \Delta t} = R^i \text{ in } d^{-1}.$$

The time $1/R^i$ is the average developmental time in days for the individuals in stage i.

We use capital letters to denote parameters that depend on temperature, and lowercase letters for those that vary with time: for instance, $V^i(T(t)) = v^i(t)$. In Brière et al. (1999); Kontodimas et al. (2004), several possible functional relationships between T and $R^i(T)$ are reported for some arthropods, from a linear relationship to more complex dependencies, such as the Brière function represented in Fig. 1. A complete and up-to-date review of thermal performance curves can be found in Kontopoulos et al. (2024).

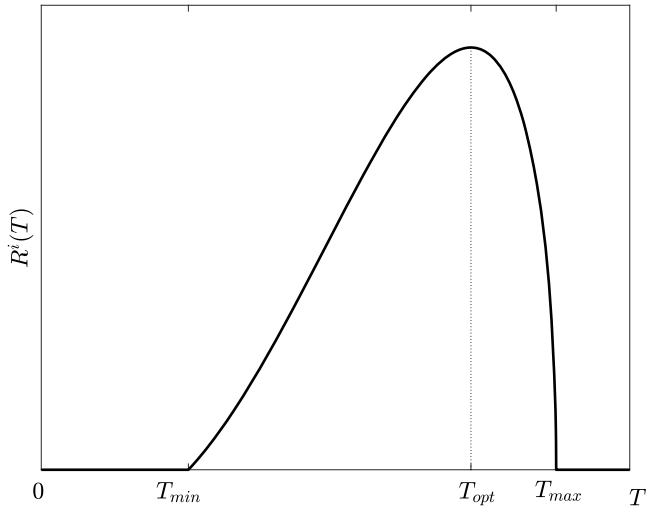

Fig. 1. Qualitative trend of a Brière development rate $R^i(T)$ vs temperature T.

Brière and Pracros (1998) state that the linear model overestimates the developmental rate at high temperatures, while at low temperatures "the linear model provides a value for the zero developmental threshold". The model's concavity at higher temperatures reflects the existence of an optimum temperature range for the development process. It is worth noting that very few experimental values are detected for temperature values greater than the optimum temperature value T^i_{opt} (Fig. 1). Arrhenius (1915) mentioned this phenomenology when dealing with the dependence of the velocity of chemical reactions on temperature: "It is a very common feature that vital and even enzymatic processes show an optimum of temperature" (Arrhenius, 1915, p. 56), and "The peculiarity that in many cases optimum temperatures are observed in life-processes or enzymatic actions are easily explained by the destructive influence of high temperatures on living cells or enzymes" (Arrhenius, 1915, p. 59). Thus, this trend should be related to the increased mortality at sufficiently high temperatures, confirmed by the data reported in Brière and Pracros (1998) regarding the number of insects completing development.

To take into account these nonlinear boundary effects, Brière and Pracros (1998) have fitted their data with different models, in particular with Logan et al. (1976) and Lactin et al. (1995) models, but obviously, the best result could not be detected. Nevertheless, whatever model for $R^i(T)$ is chosen, it should be considered acceptable only in the range of T values supported by experimental results. Brière et al. (1999) proposed the following function

$$R^i(T) = a^i T(T - T^i_{min})\sqrt{(T^i_{max} - T)}, \quad \text{for } T^i_{min} \le T \le T^i_{max}, \tag{6}$$

and $R^i(T) = 0$ for T elsewhere. The authors concluded that due to its simplicity, desirable properties, and satisfactory fit to empirical data, this development model "has a wide range of applications for insects".

3.2. Mortality rates

Let $N^i(t)$ be the average number of individuals in stage i at time t, and let $M^i(T)$ be the mortality rate of these individuals. Assume the mortality process to be described by the negative exponential equation

$$\frac{dN^i}{dt} + M^i(T)N^i = 0, \tag{7}$$

which, under a constant thermal regime, gives the survival fraction

$$\frac{N^i_{t_1}}{N^i_{t_0}} = \exp\big(-M^i(T)(t_1 - t_0)\big). \tag{8}$$

Assume $T \in (T^i_{min}, T^i_{opt})$, so that the development of the individuals is increasing. Since $N^i_{t_0}$ and $N^i_{t_1}$ are the average number of individuals entering stage i at time t_0 and leaving it at time t_1, then we should have $t_1 - t_0 = 1/R^i(T)$, so that

$$M^i(T) = -R^i(T)\ \ln\frac{N^i_{t_1}}{N^i_{t_0}}. \tag{9}$$

The survival and death of an individual are strongly affected by the temperature regime. The hazard rate function in terms of reliability is generally described by a bathtub-shaped function (Wang et al., 2002). Accordingly, the ratio between dead and initial individuals $(N^i_{t_0} - N^i_{t_1})/N^i_{t_0}$ should follow a U-shaped distribution with respect to T in the interval $T \in (T^i_{min}, T^i_{max})$. Assuming for this ratio a quadratic function

$$1 - \frac{N^i_{t_1}}{N^i_{t_0}} = U^i(T) = \left[\frac{T - T^i_{U1}}{T^i_{U2}}\right]^2, \tag{10}$$

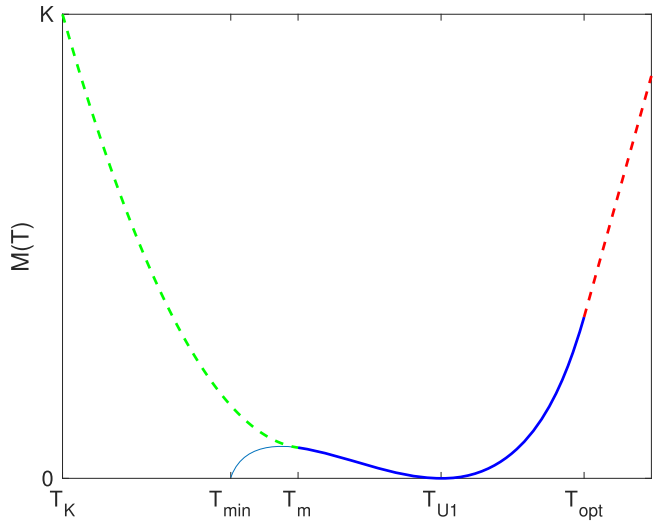

Fig. 2. Qualitative trend of the mortality rate $M^i(T)$ vs temperature T. The continuous blue line represents the mortality defined in Eq. (11) and the thin part shows the unrealistic trend near T_{min}. The red dashed line for high temperatures is the mortality defined in Eq. (12), while the green dashed line for low temperatures is defined in Eq. (14).

where T^i_{U1} and T^i_{U2} can be estimated using data on the proportion of individuals who died or survived. To avoid the proportion of dead individuals dropping to zero, a constant term can be added to Eq. (10) (see Gilioli et al. (2016)).

Then, the rate $M^i(T)$ is estimated from Eqs. (9) and (10) by

$$M^i(T) = -R^i(T)\ \ln\left(1 - U^i(T)\right), \quad T \in (T^i_{min}, T^i_{opt}). \tag{11}$$

Assuming $T^i_{opt} > T^i_{U1} > T^i_{min}$, it follows from Eqs. (10) and (11) that $M^i(T)$ is positive and increasing for $T \in \left(T^i_{U1}, T^i_{opt}\right)$. Thus, $M^i(T)$ can be linearly extrapolated for $T \geq T^i_{opt}$:

$$M^i(T) = M^i(T^i_{opt}) + a^i_0(T - T^i_{opt}), \quad T \geq T^i_{opt}, \tag{12}$$

where $a^i_0 = [d\,M^i(T)/dT]_{T=T^i_{opt}}$.

However, $M^i(T)$ given by Eq. (11) shows an unrealistic trend near T^i_{min}, i.e., increasing with T for $T \geq T^i_{min}$ (Fig. 2). Recall that the rate Eq. (11) has been obtained under the assumption Eq. (7); however, this assumption may fail near T^i_{min}. Thus, we have to confine the validity of Eq. (11) to an interval $\left(T^i_m, T^i_{opt}\right)$, with $T^i_{min} \leq T^i_m \leq T^i_{U1}$. Defining $a^i_1 = [d\,M^i(T)/dT]_{T=T^i_m}$ and

$$b^i_1 = \frac{K^i - M^i(T^i_m) - a^i_1\left(T^i_K - T^i_m\right)}{\left(T^i_K - T^i_m\right)^2} \tag{13}$$

where K^i is the value of the mortality at $T^i_K < T^i_{min}$, and can be defined according to the knowledge of the insect, $M^i(T)$ can be approximated by a second-order polynomial in $T \in (T^i_K, T^i_m)$, which is decreasing for $T > T^i_K$ and continuous at $T = T^i_m$, given by

$$M^i(T) = b^i_1(T - T^i_m)^2 + a^i_1(T - T^i_m) + M^i(T^i_m), \quad T \leq T^i_m. \tag{14}$$

Note that the resulting mortality rate is a continuous function.

3.3. Eggs production rate

The average egg production, in terms of individuals entering the egg stage, is given by the term $F^1(T)$ in (4). The egg production rate $b(t,x)$, measured in eggs/female/°C d (or eggs/female/d if the age is measured in days), is expressed as the product

$$b(t,x) = f(x)\ \alpha(\hat{T}(t))\ \beta(P(t)), \tag{15}$$

where $f(x)$ is the fecundity rate as a function of adult female age, expressed in the units eggs/female/°C d, while $\alpha(\hat{T}(t))$ is a dimensionless factor accounting for the effects of temperature. Various oviposition profiles $f(x)$ are discussed in Pasquali et al. (2019).

The factor $\alpha(\hat{T}(t))$ depends on temperature through the mean temperature value

$$\hat{T}(t) = \frac{1}{\tau}\int_{t-\tau}^{t} T(t')\,dt',$$

where τ is a suitable time interval characterizing the thermal regime influencing the physiological status of adult females.

In addition, a scaling factor $\beta(P(t))$, ranging between 0 and 1, may be introduced. This factor depends on the phenological stage $P(t)$ of the host plant, which serves as the pest's food source (Gilioli et al., 2016; Gutierrez et al., 2012). The factor $\beta(P(t))$ modulates the number of eggs laid by a female depending on the developmental stage of the host plant.

4. Diapause processes

When temperature (or its average over a given time interval) and photoperiod decrease, typically in late summer or fall, insects may enter diapause, a dormancy state that enables survival during unfavorable environmental conditions (Gill et al., 2017). Diapause occurs at a species-specific developmental stage.

Let $t_{0D}(T, P_p)$ denote the initial time of the diapause period as a function of temperature T and photoperiod P_p, and let

$$\psi(t,x)\,dx = \text{number of diapause individuals at time } t > t_{0D}.$$

Let k be the overwintering stage; then $\phi^k\,dx$ denotes the number of diapausing individuals. Assuming that diapausing individuals experience a mortality rate μ, the function $\psi(t,x)$ satisfies the equation

$$\frac{\partial\psi}{\partial t} + \mu\psi = \nu\phi^k, \quad t > t_{0D},\ \psi(t_{0D},x) = 0,$$

where the term $\nu\phi^k$ represents the rate of individuals entering diapause. Note that ν may be time-dependent and is not necessarily constant.

As temperature (or its average) increases, typically in late winter or spring, and the photoperiod lengthens, diapausing individuals resume development from the same age at which they entered diapause. Denoting this moment by $t_{1D}(T, P_p)$, we assume that the number of individuals decreases from a maximum value $\psi^* = \psi(t_{1D}, x)$ at a constant rate Υ, until it reaches zero at time t_{2D}, such that $\psi(t_{2D}, x) = 0$. From

$$\frac{\partial\psi}{\partial t} + \mu\psi = -\Upsilon, \quad t > t_{1D},\ \psi(t_{1D},x) = \psi^*,$$

it follows that

$$t_{2D} = t_{1D} + \frac{1}{\mu}\ln(1 + \mu\psi^*/\Upsilon).$$

This model can be generalized by allowing Υ to vary with time.

In general, both t_{0D} and t_{1D}, namely the times marking the onset and termination of diapause, respectively, depend on species-specific thresholds for both temperature and photoperiod and may vary from year to year.

5. The numerical approximation

A natural approach to solve the problem Eqs. (1)–(3), when $v^i(t) > 0$, is the method based on the integration of Eq. (1) along the characteristic curves $dx/dt = v^i(t)$. However, when $v^i(t)$ depends on time t, the grid step Δx related to the age variable x becomes time-dependent: $\Delta x = v^i(t)\Delta t$, where the time step Δt is assumed fixed. If the characteristic method is implemented on a grid with a time-independent age step Δx when $v^i(t)$ is time-dependent, then interpolation procedures are necessary to compute, at each time t, the unknown variable at the grid points. These numerical techniques lead to an artificial dispersion (dependent on Δx) of the individuals during the temporal evolution process.

Despite this limitation, we implement the approach with an age step Δx independent of the stage. Let the grid for the age variable x, with age step Δx, be defined by

$$x_j = j\Delta x,\ j = 0, 1, \ldots, n^i, \quad \text{with } n^i = \frac{D^i}{\Delta x}$$

and let $\phi^i_j(t) = \phi^i(t, x_j)$, $j = 1, 2, \ldots, n^i$.

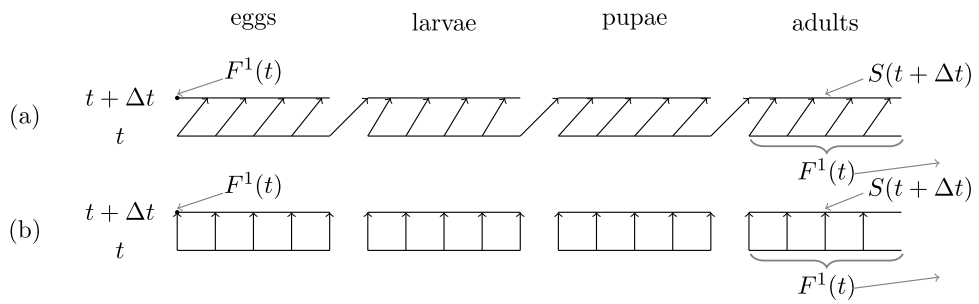

Fig. 3. Link between the variables $\phi_j^i(t)$ and $\phi_j^i(t + \Delta t)$ in the discrete equations. (a) Positive development, which allows individuals to move from one stage to the next; (b) Null development, which keeps individuals in the same stage.

Table 1
Values of $\phi_0^i(t + \Delta t)$ for $i > 1$ depending on the values of $v^{i-1}(t)$ and $v^i(t)$. In the first case, where development is zero for both stage $i - 1$ and stage i, we have only individuals already present at the previous time step, and $\phi_0^i(t + \Delta t)$ is given by formula Eq. (22). In the second case, where development is zero in stage $i - 1$ and positive in stage i, there are no individuals entering stage i at time $t + \Delta t$. In the third case, where development is positive in stage $i - 1$ and zero in stage i, at the beginning of stage i, individuals come both from the previous stage and from the current one, and $\phi_0^i(t + \Delta t)$ is given by formula Eq. (22). In the fourth case, where development is positive in both stage $i - 1$ and stage i, at the beginning of stage i, we have only individuals arriving from the previous stage, and $\phi_0^i(t + \Delta t)$ is given by formula Eq. (21).

$v^{i-1}(t)$	$v^i(t)$	$\phi_0^i(t + \Delta t)$	stage $i-1$ i
0	0	$\phi_0^i(t)\ \exp(-m^i \Delta t)$	
0	> 0	0	
> 0	0	$\phi_{n^{i-1}}^{i-1}(t)\ \exp(-m^{i-1}\Delta t) + \phi_0^i(t)\ \exp(-m^i \Delta t)$	
> 0	> 0	$\phi_{n^{i-1}}^{i-1}(t) \exp(-m^{i-1}\Delta t)\ v^{i-1}(t)/v^i(t)$	

For simplicity, in the following, we assume that at any time t we have either $v^i(t) > 0$ or $v^i(t) = 0$ for $i = 1, 2, \dots, s$. This assumption holds in some situations where T_0^i and T_L^i are weakly dependent on the stage i. Thus, the discrete equations link the variables $\phi_j^i(t)$ at the age grid points at time t with the variables $\phi_j^i(t + \Delta t)$ at the same grid points at time $t + \Delta t$, as shown in Fig. 3, for both positive ($v^i(t) > 0$) and null ($v^i(t) = 0$) development of the individuals.

The conditions that must be specified to compute $\phi_0^i(t + \Delta t)$ when $i > 1$, for arbitrary values of $v^{i-1}(t) \geq 0$ and $v^i(t) \geq 0$, are summarized in Table 1.

We observe that, when diapause is active for stage k, the developing individuals must be updated at each time t as $(1 - \nu)\phi^k \to \phi^k$.

The discrete equations associated with Eqs. (1)–(3), for both positive and null development, are given in the next subsections.

5.1. *Positive development:* $v^i(t) > 0,\ i = 1, 2, \dots, s$

Let the state variables $\phi_j^i(t)$ at time t be known, and assume the rates and the sources are constant in the time interval $(t, t + \Delta t)$ and given by their values at time t: $v^i(t)$, $m^i(t)$, $S^i(t)$. Under this assumption, the characteristic curves are straight lines in the interval $(t, t + \Delta t)$. Let us define

$$p^i(t) = \frac{v^i(t)\Delta t}{\Delta x}, \quad q^i(t) = \exp\left(-m^i(t)\Delta t\right). \tag{16}$$

We integrate Eq. (1), written as

$$\frac{d_{\mathcal{L}_j}\phi^i}{dt} + m^i(t)\phi^i(t) = S^i(t), \tag{17}$$

along the characteristic line $\mathcal{L}_j(t)$ from the point $(t, x_j - v^i(t)\Delta t)$ to $(t + \Delta t, x_j)$. To have $x_j - v^i(t)\Delta t \geq x_{j-1}$, we choose the age and time steps so that

$$p^i(t) \leq 1. \tag{18}$$

We obtain

$$\phi_j^i(t + \Delta t) = q^i(t)\phi^i(t, x_j - v^i(t)\Delta t) + \Delta t S_j^i(t).$$

By assuming a linear trend of $\phi^i(t, x)$ with x in the age interval (x_{j-1}, x_j), we obtain

$$\phi_j^i(t + \Delta t) = q^i(t)\left[p^i(t)\phi_{j-1}^i(t) + (1 - p^i(t))\phi_j^i(t)\right] + \Delta t S_j^i(t). \tag{19}$$

The boundary values $\phi_0^i(t + \Delta t) = F^i(t)$ are given by

$$F^1(t) = \sigma q^1(t)\rho\left[b(t, 0)\phi_0^s(t)\frac{\Delta x}{2} + \sum_{j=1}^{n^s-1} b(t, x_j)\phi_j^s(t)\Delta x + b(t, x_{n^s})\phi_{n^s}^s(t)\frac{\Delta x}{2}\right], \tag{20}$$

$$F^i(t) = \phi_{n^{i-1}}^{i-1}(t)q^{i-1}(t)\frac{v^{i-1}(t)}{v^i(t)}, \quad i > 1. \tag{21}$$

5.2. *Null development:* $v^i(t) = 0,\ i = 1, 2, \dots, s$

As previously mentioned, when $v^i(t) = 0$, Eq. (1) becomes an ordinary differential equation, and its solution in $(t, t + \Delta t)$ is simply written as

$$\phi_j^i(t + \Delta t) = q^i(t)\phi_j^i(t) + \Delta t S_j^i(t) + \delta_{1i}\delta_{0j}F^1(t), \quad j = 0, 1, \dots, n^s, \tag{22}$$

where $\delta_{\alpha\beta}$ is the Kronecker's δ and $F^1(t)$ is given by Eq. (20).

Table 2
(a) Estimated values of the durations D^i, of the parameters a_0^i, a_1^i, b_1^i, T_{min}^i introduced in the mortality rates Eqs. (12) and (14); (b) estimated values of the stage independent critical temperature values T_m, T_M, T_{U1}, T_{U2} (see Figs. 1 and 2) for *L. botrana*.

(a)

Parameter	Description	$i=1$	$i=2$	$i=3$	$i=4$	Unit
D^i	Average degree-day units to complete development in stage i	79	317	125	320	$°C\ d$
a_0^i	Coefficient in Eq. (12)	0.06165	0.01536	0.03896	0.01522	$(°C\ d)^{-1}$
a_1^i	Coefficient in Eq. (14)	-0.00239	-0.000596	-0.00151	-0.00059	$(°C\ d)^{-1}$
b_1^i	Coefficient Eq. (13)	0.00477	0.00502	0.00489	0.00502	$°C^{-2}\ d^{-1}$
T_{min}^i	Minimum development temperature	9.61	9.5	11.5	11.5	$(°C)$

(b)

Parameter	Description	Value	Unit
T_m	Lower limit temperature for the validity of Eq. (11)	14	$°C$
T_M	Upper limit temperature for positive linear development	33	$°C$
T_{U1}	Temperature in Eq. (10)	22.5	$°C$
T_{U2}	Temperature in Eq. (10)	12.5	$°C$

5.3. Bounds for Δt and Δx

Bounds for Δt and Δx are dictated by biological considerations. Since the rates of the main biological processes depend on time through abiotic variables, mainly through the temperature $T(t)$, the time variations of temperature should be described thoroughly in the numerical simulation of the dynamics of the whole process. The thermal diurnal cycle requires an upper bound for Δt: $\Delta t < \delta \simeq 1/12d\ (= 2\ h)$. Moreover, the technical limitation Eq. (18) must hold:

$$v^i(t)\frac{\Delta t}{\Delta x} \le \max_{i,t} v^i(t)\frac{\Delta t}{\Delta x} < 1$$

which implies an upper bound for the ratio $\Delta t/\Delta x$.

6. The case study: *Lobesia botrana*

In this section, the modelling approach presented in the previous sections is applied to the main vineyard pest in Europe: the grape berry moth *Lobesia botrana*. We consider four stages for this insect: eggs, larvae, pupae and adults. Therefore, the system Eqs. (1)–(3) becomes

$$\begin{aligned}
&\frac{\partial \phi^i}{\partial t} + V^i(T(t))\frac{\partial \phi^i}{\partial x} + M^i(T(t))\phi^i = 0, \qquad t > t_0,\ x \in (0, D^i),\ i = 1,2,3,4,\\
&\phi^1(t,0) = \sigma \int_0^{D^4} b(t,x)\ \rho \phi^4(t,x)\ dx, \qquad (23)\\
&\phi^i(t,0) = \phi^{i-1}(t, D^{i-1})V^{i-1}(T(t))/V^i(T(t)), \qquad i = 2,3,4,\\
&\phi^i(t_0,x) = \hat{\phi}^i(x), \qquad i = 1,2,3,4.
\end{aligned}$$

The grape berry moth overwinters in the pupal stage, namely $i = 3$. Moreover, we assume that the average number of females and males is equal, that is $\rho = 0.5$.
In the following, the development, mortality and fecundity functions of the grape berry moth will be made explicit to describe the behavior of different stages of the pest. We will then choose to simplify some functions to focus on describing the life cycle of the pest, without claiming to fit the abundance data collected in the field, but to get an idea of the population cycle.

Development. In Gilioli et al. (2016), the development rate functions $R^i(T)$ for the different stages of the grape berry moth are represented by Lactin functions. Since the increasing part of this rate is well approximated by a linear function, we can consider the development rates

$$R^i(T) = \frac{T(t) - T_{min}^i}{D^i}\ (d^{-1}), \quad V^i(T) = T(t) - T_{min}^i\ (°C), \quad \text{for } T_{min}^i < T(t) \le T_M, \qquad (24)$$

and zero elsewhere, where T_M is a value between the optimal and the maximum development temperatures. Linear development rate functions are also used in Kettle et al. (2024).

To determine the values of D^i, that is the average degree-days needed to complete the development in a stage, for immature individuals, we consider the linear fit of the development data in Baumgaertner and Baronio (1988); Brière and Pracros (1998), used to obtain the Lactin function in Gilioli et al. (2016), up to $T_M = 33°C$. The upper temperature limit of the straight line can be chosen based on available development rate data and abundance data collected in the field for different stages. The inverse of the straight line slope represents the average degree-days D^i needed to complete development in stage i; values of D^i are reported in Table 2 and are in agreement with those calculated in Gutierrez et al. (2012).

The age of the adult females is obtained from the fecundity rate function proposed by Baumgaertner and Baronio (1988). The production of eggs by an adult female is negligible after $320°Cd$, so we consider this value as the maximum age D^4 for an adult female (Table 2).

The straight lines describing the development rate give a minimum development temperature of $9.61°C$ for eggs, $9.5°C$ for larvae and $11.5°C$ for pupae (Table 2). For adults, we consider the same minimum development temperature as for pupae.

Mortality. Recall the mortality rate function

$$M^i(T) = \begin{cases} -R^i(T_m)\ln\left[1 - U(T_m)\right] + b_1^i(T - T_m)^2 \\ \quad + a_1^i(T - T_m), & T < T_m \\ -R^i(t)\ln\left[1 - U(T)\right], & T_m \le T \le T_{opt} \\ -R^i(T_{opt})\ln\left[1 - U(T_{opt})\right] + a_0^i(T - T_{opt}), & T > T_{opt} \end{cases}$$

with

$$U(T) = \left[\frac{T - T_{U1}}{T_{U2}}\right]^2$$

$$a_0^i = \left[\frac{d}{dT}\left[-R^i(t)\ln\left[1 - U(T)\right]\right]\right]_{T=T_{opt}},$$

$$a_1^i = \left[\frac{d}{dT}\left[-R^i(t)\ln\left[1 - U(T)\right]\right]\right]_{T=T_m},$$

and b_1^i defined in Eq. (13). For the sake of simplicity, we chose the same values of T_m, T_{U1} and T_{U2} for all the stages (Table 2). We are aware that parameters in $U(T)$ are also stage-dependent, but as mentioned earlier, we simplify some functions to focus on pest cycle behavior. In any case, we consider reasonable parameters according to models in the literature (Gilioli et al., 2016).

Table 3
Estimated values of the parameters introduced in the eggs production rate $b(t,x)$ in Eq. (25) for *L. botrana* (see Baumgaertner and Baronio (1988) and Gutierrez et al. (2012)). (a) parameters of the fecundity rate function Eq. (25); (b) definition of the step function $\beta(P(t))$ representing a scaling factor for fecundity.

(a)

Parameter	Description	Value	Unit
x_0	Minimum adult age for reproduction	16	$°C\ d$
c_1	Coefficient in Eq. (25)	1.4176	eggs/female/$(°C d)^2$
c_2	Coefficient in Eq. (25)	0.0251	$(°C\ d)^{-1}$
τ	n. of days for the average temperature $\hat{T}$	10	d
$\hat{T}_1$	Temperature in Eq. (25)	24.5	$°C$
$\hat{T}_2$	Temperature in Eq. (25)	7.5	$°C$

(b)

Plant stage	Value of $P(t)$	Scaling factor
Inflorescence	$P(t)=1$	$\beta(1)=0.31$
Green berries	$P(t)=2$	$\beta(2)=0.48$
Maturing fruits	$P(t)=3$	$\beta(3)=1$

Table 4
Lobesia botrana: average developmental times for eggs, larvae, pupae, life span for adults, and mortality rates, for all stages, at $T = 20\ °C$.

stage	$1/R^i\ (d)$	$M^i\ (d^{-1})$
Eggs	7.6	0.005369
Larvae	30.2	0.001352
Pupae	14.7	0.002776
Adults	37.6	0.001084

Table 5
$\log_{10} N^4$ at time $t = 3y$ vs. ϵ. $\Delta t = 1/24d$, $\Delta x = 2°Cd$.

$\log_{10}\epsilon$	-1	-1.3	-2	-3	-4	-6
$\log_{10} N^4$	1.4	1.7	2.4	3.4	4.4	6.4

The parameters of the mortality function defined in Eqs. (12)–(14) for low and high temperature values are reported in Table 2, for $K^i = 1$ $(i = 1,2,3,4)$ at $T_K = 0$.

Fecundity. The parameters of egg production rate

$$b(t,x) = c_1\left(x - x_0\right)e^{-c_2\left(x-x_0\right)}\left[1 - \left(\frac{\hat{T} - \hat{T}_1}{\hat{T}_2}\right)^2\right]\beta(P(T)) \tag{25}$$

are reported in Table 3 and come from Baumgaertner and Baronio (1988) and Gutierrez et al. (2012). The egg production rate is a function of the average temperature $\hat{T}$ over the last 10 days, i.e. $\tau = 10\ d$.

In real-world situations, the environment temperature is obviously time-dependent, and it may also vary rapidly with time. Nevertheless, it is worth considering first the ideal case of a constant and favourable temperature regime, in which $v^i > 0$ (positive development of the individuals in any stage and at any time). This scenario allows us to estimate the numerical effects due to variations of the two parameters Δx, Δt, on the dynamics of the system, and to enlighten the response of the model in the absence of possible control due to the variability of the environmental conditions.

6.1. Constant temperature without diapause

Assuming a constant temperature $T = 20°C$, favorable for insect growth, the average developmental times $1/R^i(T) = D^i/(T - T_0)$ and the rates $M^i(T) = -R^i \ln(1 - U(T))$ for the sample population *Lobesia botrana* are given in Table 4.

By considering the values in Table 3, we obtain $\alpha(T) = 0.64$; moreover, we choose $\beta(P(t)) = 0.5$ (mean value of the range $[0,1]$ of variability of $\beta(P(t))$ in the rate of egg production Eq. (25), so that $b(x) = 0.32 \cdot f(x)$. The scenario of constant temperature $T = 20°C$ with a linear system of evolution Eqs. (1)–(5) (with σ constant in Eq. (4)), i.e. without any explicit control feedback of the population on its growth, is discussed in the Appendix.

Let us now assume the factor σ in Eq. (23) to be dependent on some characteristic $z(t)$ of the population (Bergh and Getz, 1988; Buffoni and Pasquali, 2007): e.g. $z(t) = N(t)$ is the overall population size or $z(t) = N^4(t)$ is the adult abundance. The control function $\sigma(z)$ may be either a decreasing or a unimodal function of z (Buffoni and Pasquali, 2007), and it provides the basic control of the population on the recruitment, and then on the population growth. The existence and stability of steady-state solutions to the discrete problem Eqs. (19)–(22) hold under suitable conditions (see Buffoni and Pasquali (2007)). Numerical experiments have been performed with $T = 20°C$, $\sigma(N) = \exp(-\epsilon N)$, and for different ϵ, Δt, Δx. The initial condition is 50 adults uniformly distributed over the age, that is $\phi_j^i(0) = 0,\ i = 1,2,3,\ \forall j;\quad \phi_j^4(0) = 50/(n^4\,\Delta x),\ \forall j$. Positive equilibrium states exist for $\epsilon > 0$. As $\epsilon \to 0$, the population fast increases (see Table 5), and an equilibrium state is attained with damped oscillations in about three years (a period that slightly increases for small ϵ).

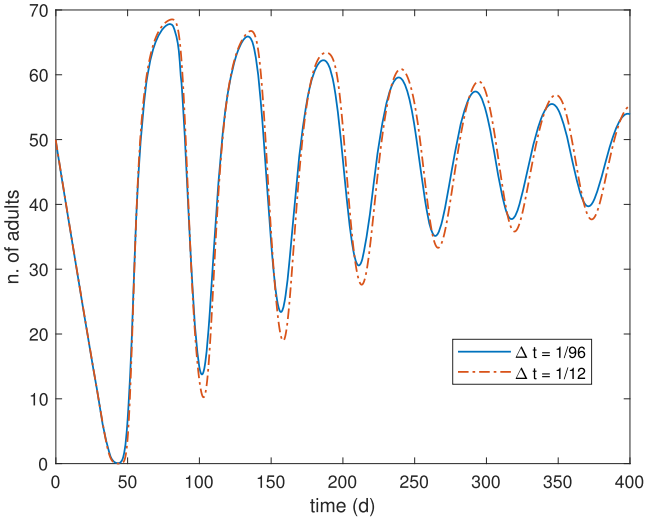

Fig. 4. Dynamics of adults of *L. botrana* with constant temperature $T = 20°C$, no diapause, when $\sigma(N) = \exp(-\epsilon N)$, for $\epsilon = 0.05$, $\Delta x = 2\ °Cd$, $\Delta t = 1/96\ d$ (blue continuous line), $\Delta t = 1/12$ (red dashed-dotted line). Initial condition of 50 adults uniformly distributed over the age.

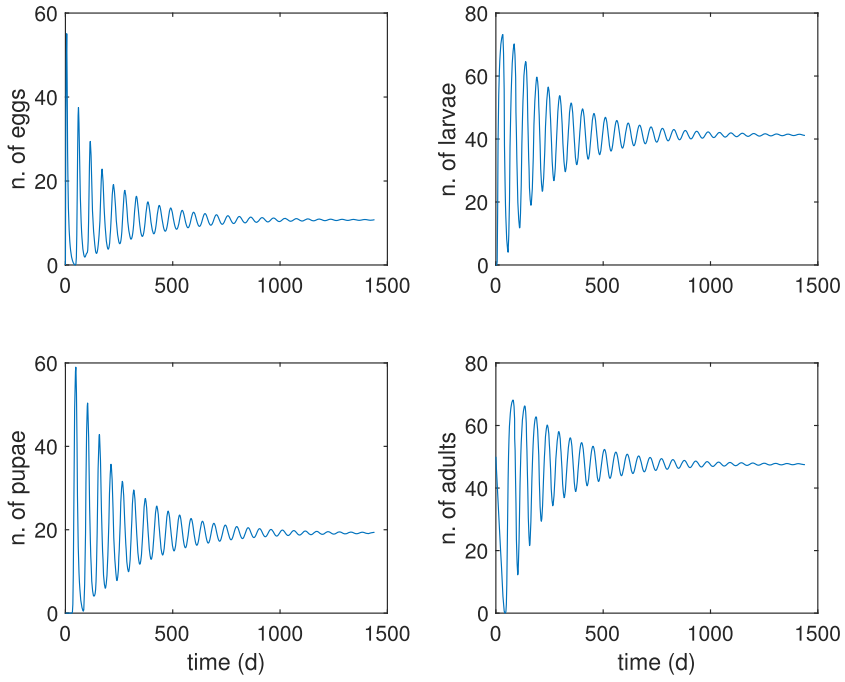

Fig. 5. Dynamics of eggs, larvae, pupae and adults of *L. botrana* with constant temperature $T = 20^oC$, no diapause, when $\sigma(N) = \exp(-\epsilon N)$ for $\epsilon = 0.05$, $\Delta t = 1/24\ d$, $\Delta x = 2\ ^oCd$. Initial condition of 50 adults uniformly distributed over the age.

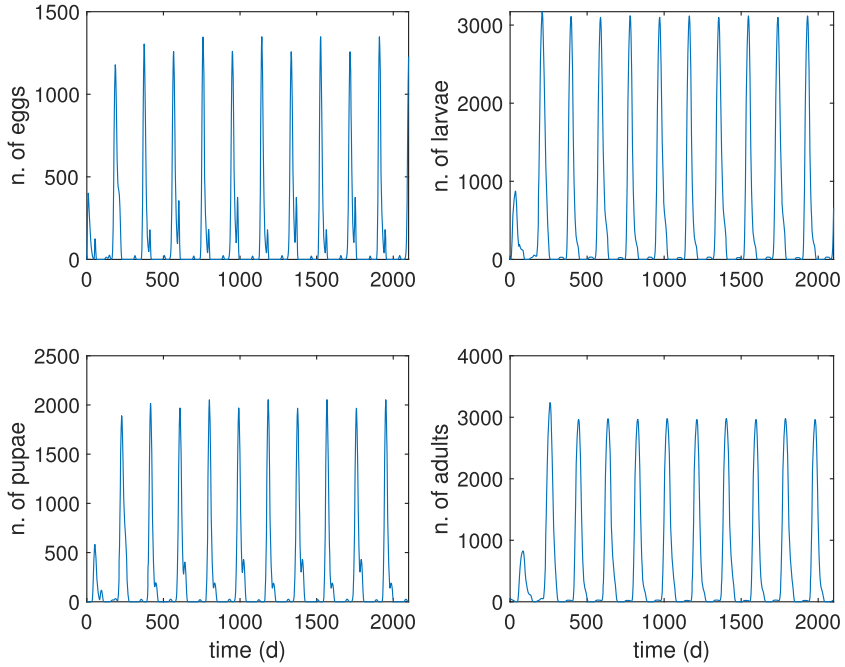

Fig. 6. Dynamics of eggs, larvae, pupae and adults of *L. botrana* with constant temperature $T = 20^oC$, no diapause, when $\sigma(N) = \exp(-\epsilon N^4)$ for $\epsilon = 0.05$, $\Delta t = 1/24\ d$, $\Delta x = 2\ ^oCd$. The initial condition of 50 adults uniformly distributed over the age.

Under the assumptions made in this subsection, condition Eq. (18) becomes $v^i \Delta t/\Delta x \leq 1$. The choice $v^i \Delta t/\Delta x = 1$ corresponds to the method of characteristics for which no interpolations are needed (i.e., $x_j - v^i \Delta t = x_{j-1}$).

For both $\Delta x = 1°Cd$ and $\Delta x = 2°Cd$, numerical simulations have been performed for the following Δt:

$\Delta t = 1/96\ d$ (0.25 h), $1/48\ d$ (0.5 h), $1/24\ d$ (1 h), $1/12\ d$ (2 h).

The peaks for pupae and adults for the different generations, for $\epsilon = 0.05$, are weakly sensitive to $\Delta t \in [0.25h, 2h]$, as shown in Fig. 4, where the differences between the adult dynamics for the two extreme cases $\Delta t = 1/96$ and $\Delta t = 1/12$, for $\Delta x = 2°Cd$, are reported. Moreover, the equilibrium state is not affected by Δt.

When fecundity depends on the overall population density, i.e., $\sigma(N) = \exp(-\epsilon N)$ with $\epsilon = 0.05$, $\Delta t = 1/24\ d$, and $\Delta x = 2\ ℃\ d$ (Fig. 5),

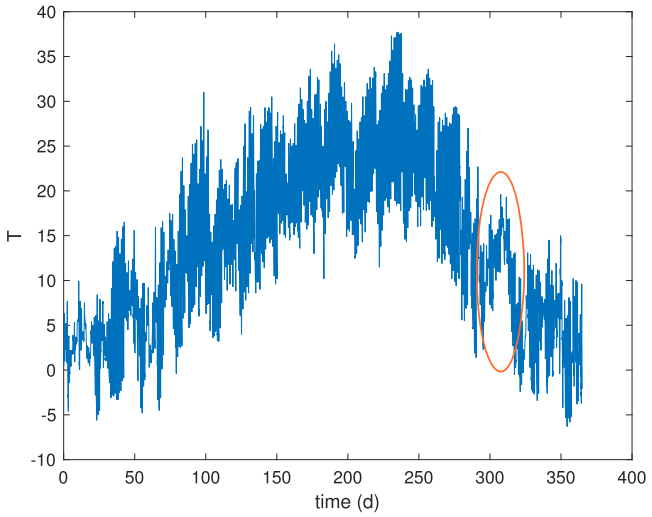

Fig. 7. Hourly temperatures in Conselice (RA), Emilia Romagna region, Italy, year 2011. The orange ellipse denotes the anomalous peak in November.

the population dynamics converge to a steady state characterized by 10.39 eggs, 40.58 larvae, 19.86 pupae, and 49.9 adults.

If a density-dependent fecundity rate is considered with control acting only on the adult population, i.e., $\sigma(N) = \exp(-\epsilon N^4)$, the dynamics of all developmental stages exhibit periodic behavior, and the steady state becomes unstable (Fig. 6).

6.2. Variable temperature and diapause

In general, it can be observed that a variable temperature regime fails to control the fast growth when $\sigma = 1$ in Eq. (4). Therefore, we consider a density-dependent egg production (Bergh and Getz, 1988; Buffoni and Pasquali, 2007). When $\sigma(N) = \exp(-0.05N)$, starting from an initial population on April 10, consisting of 50 adults uniformly distributed over the physiological age, and using a set of hourly temperatures collected in 2011 in Conselice (RA), Emilia Romagna region (shown in Fig. 7), we obtain the population dynamics represented in Fig. 8 for $\Delta t = 1/24\ d$ and $\Delta x = 2\ ^oCd$.

The results show three annual generations of the grape berry moth, which is consistent with the known biology of *L. botrana*, typically exhibiting 3 to 4 generations per year. The dependence of fecundity on the total population effectively limits excessive growth. The population dies out in late fall when temperatures drop to low values. Pupae and adults persist until early November, likely due to an anomalous temperature peak during this period (highlighted in Fig. 7).

Next, we introduce diapause. In Roditakis and Karandinos (2001), the authors conducted a series of experiments in which grape berry moth eggs and larvae were exposed to different photoperiods at 20^oC, and found that the percentage of diapausing pupae increased below $14.15\ h$ as the photoperiod P_p decreased. Following this, we assume that diapause is induced by an average temperature over the past 48 hours below 20^oC, and that ν is a function of time through the photoperiod P_p, as in Gutierrez et al. (2012):

$$\nu(P_p(t)) = \begin{cases} \min\left\{0.46\,(14.15 - P_p), 1\right\} & P_p \le 14.15, \\ 0 & \text{otherwise.} \end{cases} \tag{26}$$

We assume a constant mortality rate for diapausing individuals, $\mu = 0.005\ d^{-1}$, and a constant diapause exit rate $\Upsilon = 0.005/\Delta t\ d^{-1}$. Pupae terminate diapause when the average temperature over the previous 48 hours exceeds 11.5^oC (see Gutierrez et al. (2012)) and the photoperiod $P_p > 14.15$. We simulate the dynamics for $\Delta t = 1/24\ d$ and $\Delta x = 2^oCd$ over two years, starting from the same initial condition as in the previous case. Since the aim is to show the output of our model when diapause is included, without aiming to reproduce specific field data, the two-year temperature set is generated by repeating the temperatures from 2011 in Conselice (RA). The resulting dynamics are shown in Fig. 9. For longer periods (e.g., five years) using the same cycled 2011 temperature data, the dynamics converge to an annual pattern consisting of three generations, matching the second year results in Fig. 9. By increasing the value

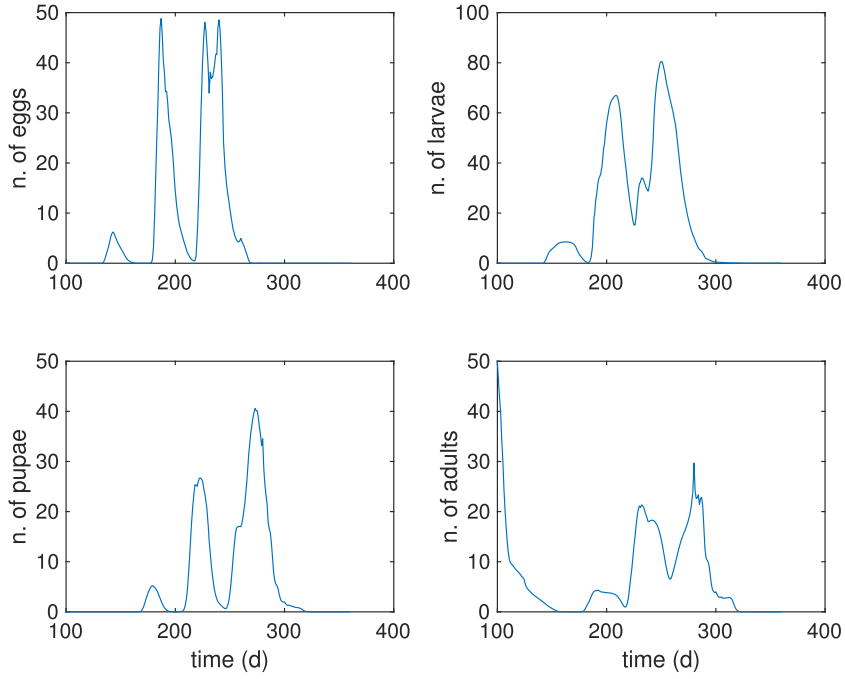

Fig. 8. Dynamics of eggs, larvae, pupae and adults of *L. botrana* in Conselice (RA), Emilia Romagna region, Italy, using temperatures of the year 2011 represented in Fig. 7. Initial condition at April 10, (day 100) of $N^4(0) = 50$ adults uniformly distributed over the physiological age, $\Delta x = 2^oCd$, $\Delta t = 1/24\,d$, $\sigma(N) = \exp(-0.05N)$, no diapause.

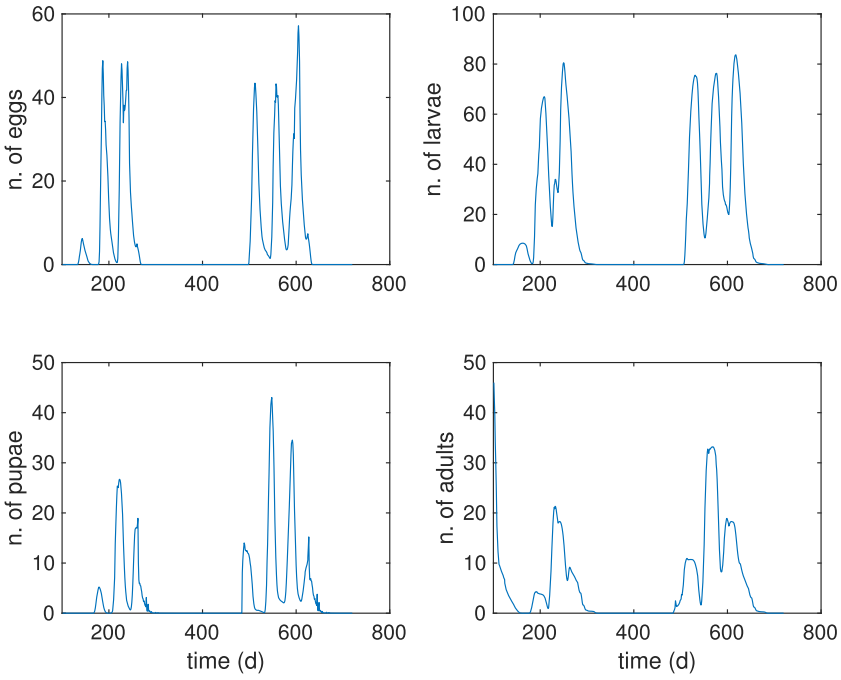

Fig. 9. Dynamics of eggs, larvae, pupae and adults of *L. botrana* in Conselice (RA), Emilia Romagna region, Italy, when considering diapause. Temperatures are obtained by cycling the temperature in Fig. 7 for two years. Time 0 is January 1st. Initial condition at April 10, (day 100) of $N^4(0) = 50$ adults uniformly distributed over the physiological age, $\Delta x = 2^oCd$, $\Delta t = 1/24\,d$, $\sigma(N) = \exp(-0.05N)$.

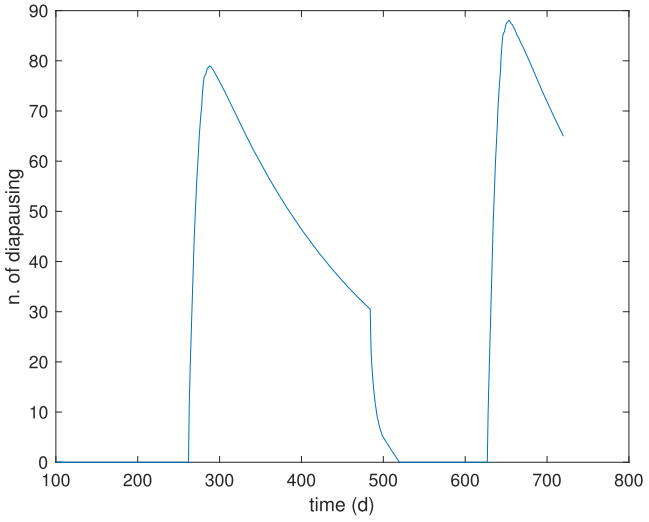

Fig. 10. Dynamics of diapausing pupae of *L. botrana* in Conselice (RA), Emilia Romagna region, Italy. Temperatures are obtained by cycling the temperature in Fig. 7 for two years. Time 0 is January 1st. Initial condition at April 10, (day 100) of $N^4(0) = 50$ adults uniformly distributed over the physiological age, $\Delta x = 2^oCd$, $\Delta t = 1/24\,d$, $\sigma(N) = \exp(-0.05N)$.

of ϵ, the three generations overlap more, although the total number of generations remains unchanged. The number of diapausing individuals (pupae) over time is shown in Fig. 10.

By comparing Figs. 8 and 9, we observe that the pupal peak in fall is significantly attenuated by diapause, as is the all adult peak. Diapausing pupae resume development at the end of April of the following year. As shown in Fig. 10, diapausing pupae peak around late October and then decrease due to mortality until late April, when diapause exit begins. This exit accelerates the decline, which continues until the end of May.

7. Concluding remarks

In this work, a demographic model is presented that integrates several crucial processes regulating the life of an insect population. The model is based on a system of partial differential equations governed by development, mortality, and fecundity rate functions. While development and fecundity parameters can often be estimated from literature data on the species' biology, laboratory data on mortality rates are frequently lacking. Consequently, we propose a functional form for the mortality rate that depends on the development rate function and on the proportion of individuals dying during each stage.

The model has been employed to simulate the dynamics of the grape berry moth. Without incorporating any population control feedback on its growth, i.e., for $\sigma = 1$, both under a constant temperature regime favourable to insect growth ($T \simeq 20°C$) and under realistic environmental conditions $T \in (\simeq 5°C, \simeq 35°C)$, population growth remained uncontrolled. This highlighted the necessity of introducing a feedback control mechanism regulating population growth within the model equations. This can be effectively achieved through a control of the total population affecting recruitment (Bergh and Getz, 1988; Buffoni and Pasquali, 2007). In Gilioli et al. (2016), to prevent population explosion, an additional mortality term was incorporated, whereas in Pasquali et al. (2022), mortality was modelled as a linear combination of cubic splines, with coefficients estimated from grape berry moth population dynamics. Here, to regulate the population, a density-dependent term, depending either on adults or on the entire population, is introduced in the fecundity rate function. Under constant temperature conditions, when the additional term depends on the entire population, the dynamics converge to a steady-state solution, while dependence solely on the adult stage results in periodic behaviour.

Furthermore, numerical simulations under constant temperature conditions indicate that the peaks for pupae and adults are only marginally influenced by the timestep Δt, whereas the equilibrium state remains independent of Δt. Minor variations in peak magnitudes are also observed for different spatial discretizations Δx over time.

An additional significant contribution of this work is the precise formulation and integration of the diapause process into the PDE model, thereby enabling simulations of pest dynamics over multiple years. The overwintering process is regulated by temperature and photoperiod. We assume that individuals enter diapause when both the photoperiod and the average temperature over a specified time interval fall below critical thresholds. The diapause process attenuates the fall peaks of pupae and adults and permits a resumption of population dynamics in the subsequent spring. This advancement facilitates long-term simulation of pest populations (not limited to *L. botrana*) and, crucially, allows prediction of spring dynamics in advance based on temperature data, thus informing targeted field data collection guided by model forecasts.

CRediT authorship contribution statement

Giuseppe Buffoni: Writing – review & editing, Writing – original draft, Methodology, Formal analysis, Conceptualization; **Sara Pasquali:** Writing – review & editing, Writing – original draft, Methodology, Formal analysis, Conceptualization; **Cinzia Soresina:** Writing – review & editing, Writing – original draft, Methodology, Formal analysis, Conceptualization.

Declaration of competing interest

The authors declare that they have no known competing financial interests or personal relationships that could have appeared to influence the work reported in this paper.

Acknowledgements

CS is a member of INdAM-GNFM.
The authors are grateful to two anonymous reviewers for their helpful comments that allowed improving the manuscript.

Appendix A. Appendix - the time evolution of the linear system under the assumption $T = 20°C$ and σ constant

Under the assumptions made in Section 3.1 on the developmental rate, from Eq. (24), the rate v is in $°C$ and is stage-independent. Thus, the quantities $p^i(t)$ and $q^i(t)$ in Eq. (16) are given here by

$$p^i = \frac{v^i \Delta t}{\Delta x}, \quad q^i = \exp\left(-m^i \Delta t\right).$$

In the case of positive development with constant coefficients, and null sources, the linear (σ constant) discrete Eqs. (19)–(21) are written as

$$\phi^i_j(t+\Delta t) = q^i\left[p^i \phi^i_{j-1}(t) + (1-p^i)\phi^i_j(t)\right], \tag{A.1}$$

while the boundary values $\phi^i_0(t+\Delta t) = F^i(t)$ are given by

$$F^1(t) = \sigma q^1 \rho\left[b_0 \phi^s_0(t)\frac{\Delta x}{2} + \sum_{j=1}^{n^s-1} b_j \phi^s_j(t)\Delta x + b_{n^s}\phi^s_{n^s}(t)\frac{\Delta x}{2}\right], \tag{A.2}$$

$$F^i(t) = \phi^{i-1}_{n^{i-1}}(t) q^{i-1}\frac{v^{i-1}}{v^i} = \phi^{i-1}_{n^{i-1}}(t)q^{i-1} \quad i > 1. \tag{A.3}$$

Let the vector $\varphi^i(t)$ be defined as

$$\varphi^i(t) = [\phi^i_0(t), \phi^i_1(t), \dots, \phi^i_{n^i}(t)].$$

Eqs. (A.1)–(A.3) are written in vector form as

$$\varphi^1(t+\Delta t) = A^1\varphi^1(t) + \sigma B^4 \varphi^4(t),$$

$$\varphi^i(t+\Delta t) = B^{i-1}\varphi^{i-1}(t) + A^i\varphi^i(t), \quad i = 2,3,4.$$

Let A^i be the matrices given by

$$A^i = \begin{vmatrix} 0 & 0 & 0 & \dots & 0 & 0 & 0 \\ q^i p^i & q^i(1-p^i) & 0 & \dots & 0 & 0 & 0 \\ 0 & q^i p^i & q^i(1-p^i) & \dots & 0 & 0 & 0 \\ \dots & \dots & \dots & \dots & \dots & \dots & \dots \\ \dots & \dots & \dots & \dots & \dots & \dots & \dots \\ 0 & 0 & 0 & \dots & q^i p^i & q^i(1-p^i) & 0 \\ 0 & 0 & 0 & \dots & 0 & q^i p^i & q^i(1-p^i) \end{vmatrix}.$$

Moreover, the entries of the matrices B^i are zero except: the first row of B^4, given by

$$q^1 \rho \Delta x[0.5b_0, b_1, \dots, b_{n^s-1}, 0.5b_{n^s}],$$

and the entry $(1, n^i)$ of B^i, $i = 1,2,3$, given by $q^{i-1}v^{i-1}/v^i = q^{i-1}$. The iteration matrix is

$$\mathcal{M} = \begin{vmatrix} A^1 & O & O & \sigma B^4 \\ B^1 & A^2 & O & O \\ O & B^2 & A^3 & O \\ O & O & B^3 & A^4 \end{vmatrix},$$

and it is a non-negative irreducible matrix. Let μ_1 and μ_2 be the minimum and maximum of the sum of the entries of each row of $\mathcal{M}$

$$\mu_1 = \min[q^i,\ q^1 E] \quad \mu_2 = \max[q^i,\ q^1 E],$$

where

$$E(\sigma) = \sigma\rho\Delta x\left(0.5b_0 + \sum_{j=1}^{j=n^s-1} b_j + 0.5b_{n^s}\right).$$

Then the spectral radius $\lambda(\sigma)$ of $\mathcal{M}$ satisfies $\mu_1(\sigma) \le \lambda(\sigma) \le \mu_2(\sigma)$ and it is increasing with σ (Varga (1962), p.20). The iterative process, governed by $\lambda(\sigma)$, is essentially the power method applied to the matrix $\mathcal{M}$. With the parameter values given in Section 6.1 for $T = 20°C$, and $\Delta x = 2$, $\Delta t = 1/24$, we obtain the parameters in Table A.6.

Table A.6
Parameters p^i and q^i in formula Eq. (16).

stage	p^i	q^i
1	0.2164583	0.9997763
2	0.21875	0.9999437
3	0.177083	0.9998843
4	0.177083	0.9999548

With $\sigma = 1$ the number of eggs is $E = 357.6426$, consequently $\mu_1 = 0.9998$ and $\mu_2 = 357.6247$. Numerical simulations produce a fast divergent process, showing that $\lambda \gg 1$. With $\sigma = 0.002615$ the number of eggs is 0.8458 and the dynamics converge to a steady state.

References

Abia, L.M., Angulo, O., Lopez-Marcos, J.C., 2004. Size-structured population dynamics models and their numerical solutions. Discret. Contin. Dynam. Syst. Ser. B 4, 1203–1222.
Angulo, O., Lopez-Marcos, J.C., 2004. Numerical integration of fully nonlinear size-structured population models. Appl. Numer. Math. 50, 291–327.
Arrhenius, S., 1915. Quantitative Laws in Biological Chemistry. G.Bell and sons.
Baumgaertner, J., Baronio, P., 1988. Modello fenologico di volo di Lobesia botrana Den. & Schiff. (Lep. Tortricidae) relativo alla situazione ambientale della Emilia Romagna. Bollettino dell'Istituto di Entomologia "G. Grandi" dell'Università di Bologna 43, 157–170.
Bergh, M.O., Getz, W.M., 1988. Stability of discrete age-structured and aggregated delay-difference population models. J. Math. Biol. 26, 551–581.
Bhagarathi, L.K., Maharaj, G., 2023. Impact of climate change on insect biology, ecology, population dynamics, and pest management: a critical review. World J. Adv. Res. Rev. 19 (3), 541–568.
Brière, J.F., Pracros, P., 1998. Comparison of temperature-dependent growth models with the development of Lobesia botrana (Lepidoptera: Tortricidae). Environ. Entomol. 27 (1), 94–101.
Brière, J.F., Pracros, P., Roux, A.Y., Pierre, J.S., 1999. A novel rate model of temperature-dependent development for arthropods. Environ. Entomol. 28 (1), 22–29.

Buffoni, G., Pasquali, S., 2007. Structured population dynamics: continuous size and discontinuous stage structures. J. Math. Biol. 54, 555–595.
Buffoni, G., Pasquali, S., 2010. Individual-based models for stage structured populations: formulation of "no regression" development equations. J. Math. Biol. 60 (6), 831–848.
Buffoni, G., Pasquali, S., 2013. On modeling the growth dynamics of a stage structured population. Int. J. Biomath. 6 (06), 1350039.
Buffoni, G., Pasquali, S., Soresina, C., 2025. Revisiting a Demographic Model of Pest Infestation in Farming. 31.03. https://github.com/soresina/BuffoniPasqualiSoresina2025.
Cabi, 2014. Lobesia botrana (grape berry moth). In: CABI Invasive Species Compendium. http://www.cabi.org/isc/datasheet/42794.
Curry, G.L., Feldman, R.M., 1987. Mathematical foundations of population dynamics. Texas A & M University Press.
Ewing, D.A., Blok, V., Kettle, H., 2021. A process-based, stage-structured model of potato cyst nematode population dynamics: effects of temperature and resistance. J. Theoret. Biol.J. Theor. Biol. 522, 110701.
Getz, W.M., Gutierrez, A.P., 1982. A perspective on systems analysis in crop production and insect pest management. Annu. Rev. Entomol. 27 (1), 447–466.
Gilioli, G., Pasquali, S., Marchesini, E., 2016. A modelling framework for pest population dynamics and management: an application to the grape berry moth. Ecol. Modell. 320, 348–357.
Gill, H.K., Goyal, G., Chahil, G., 2017. Insect diapause: a review. J. Agricult. Sci. Technol. A 7, 454–473.
Gutierrez, A.P., Ponti, L., Cooper, M.L., Gilioli, G., Baumgaertner, J., Duso, C., 2012. Prospective analysis of the invasive potential of the european grapevine moth Lobesia botrana (Den. & Schiff.) in California. Agric. For. Entomol. 14, 225–238.
Hoppenstaedt, F., 1975. Mathematical theories of populations: Demographics, genetics and epidemics. SIAM.
Kettle, H., Ewing, D.A., Coston, D., White, S., Pope, T., Roberts, J.M., 2024. A process-Based life cycle of the cabbage stem flea beetle on winter oilseed rape: Effects of temperature. SSRN 5021348.
Kontodimas, D.C., Eliopoulos, P.A., Stathas, G.J., Economou, L.P., 2004. Comparative temperature-dependent development of Nephus includens (Kirsch) and Nephus bisignatus (Boheman)(Coleoptera: Coccinellidae) preying on Planococcus citri (Risso)(Homoptera: Pseudococcidae): evaluation of a linear and various nonlinear models using specific criteria. Environ. Entomol. 33 (1), 1–11.
Kontopoulos, D.G., Sentis, A., Daufresne, M., Glazman, N., Dell, A.I., Pawar, S., 2024. No universal mathematical model for thermal performance curves across traits and taxonomic groups. Nat. Commun. 15 (1), 8855.
Kooi, B.W., Kelpin, F. D.L., 2003. Physiologically structured population dynamics: a modeling perspective. Comment. Theoret. Biol. 8 (2–3), 125–168.
Kumar, R., Rathor, V.S., 2020. Nature and types of damage by insect pests. J. Entomol. Res. 44 (4), 639–646.
Lactin, D.J., Holliday, N.J., Johnson, D.L., Craigen, R., 1995. Improved rate model of temperature-dependent development by arthropods. Environ. Entomol. 24, 68–75.
Lanzarone, E., Pasquali, S., Gilioli, G., Marchesini, E., 2017. A bayesian estimation approach for the mortality in a stage-structured demographic model. J. Math. Biol. 75, 759–779.
Logan, J.A., Wollkind, D.J., Hoyt, S.C., Tanigoshi, L.K., 1976. An analytic model for description of temperature dependent rate phenomena in arthropods. Environ. Entomol. 5, 1133–1140.
Lou, Y., Liu, K., He, D., Gao, D., Ruan, S., 2019. Modelling diapause in mosquito population growth. J. Math. Biol. 78 (7), 2259–2288.
Lou, Y., Sun, B., 2022. Stage duration distributions and intraspecific competition: a review of continuous stage-structured models. Math. Biosci. Eng. 19 (7), 7543–7569.
Manly, B.F., 1990. Stage-Structured Populations: Sampling, Analysis and Simulation. Springer, Netherlands.
Mcnair, J.N., 1995. Ontogenetic patterns of density-dependent mortality: contrasting stability effects in populations with adult dominance. J. Theor. Biol. 175 (2), 207–230.
Murdoch, W.W., Briggs, C.J., 1996. Theory for biological control: recent developments. Ecology 77 (7), 2001–2013.
Murphy, L.F., 1983. A nonlinear growth mechanism in size structured population dynamics. J. Theor. Biol. 104 (4), 493–506.
Pak, D., Carran, S., Biddinger, D., Nelson, B., rnstad, O. N.B., 2022. Incorporating diapause to predict the interannual dynamics of an important agricultural pest. Popul. Ecol. 64 (3), 267–279.
Pasquali, S., 2021. A stage structured demographic model with "no-regression" growth: the case of constant development rate. Physica A 581, 126200.
Pasquali, S., Soresina, C., Gilioli, G., 2019. The effects of fecundity, mortality and distribution of the initial condition in phenological models. Ecol. Modell. 402, 45–58.
Pasquali, S., Soresina, C., Marchesini, E., 2022. Mortality estimate driven by population abundance field data in a stage-structured demographic model. The case of Lobesia botrana. Ecol Modell 464, 109842.
Pasquali, S., Trivellato, B., 2023. A stage structured demographic model with "no-regression" growth: the case of temperature-dependent development rate. Physica A 629, 129179.
Pawar, S., Huxley, P.J., Smallwood, T.R., Nesbit, M.L., Chan, A.H., Shocket, M.S., Johnson, L.R., Kontopoulos, D., Cator, L.J., 2024. Variation in temperature of peak trait performance constrains adaptation of arthropod populations to climatic warming. Nat. Ecol. Evolut. 8 (3), 500–510.
Roditakis, N.E., Karandinos, M.G., 2001. Effects of photoperiod and temperature on pupal diapause induction of grape berry moth Lobesia botrana. Physiol. Entomol. 26 (4), 329–340.
Rossini, L., Bruzzone, O.A., Contarini, M., Bufacchi, L., Speranza, S., 2022. A physiologically based ode model for an old pest: modeling life cycle and population dynamics of Bactrocera oleae (Rossi). Agronomy 12 (10), 2298.
Rossini, L., Bruzzone, O.A., Speranza, S., Delfino, I., 2023. Estimation and analysis of insect population dynamics parameters via physiologically based models and hybrid genetic algorithm MCMC methods. Ecol. Inform. 77, 102232.
Sperandio, G., Pasquali, S., Pradolesi, G., Baiocco, S., Cavina, F., Gilioli, G., 2024. An empirical model for predicting insects diapause termination and phenology: an application to Cydia pomonella. J. Appl. Entomol. 148 (10), 1276–1291.
Subedi, B., Poudel, A., Aryal, S., 2023. The impact of climate change on insect pest biology and ecology: implications for pest management strategies, crop production, and food security. J. Agricult. Food Res. 14, 100733.
Sulsky, D., 1994. Numerical solution of structured population models: II mass structure. J. Math. Biol. 32, 491–514.
Varga, R.S., 1962. Matrix Iterative Analysis. Englewood Cliffs, Prentice-Hall.
Wang, K.S., Hsu, F.S., Liu, P.P., 2002. Modeling the bathtub shape hazard rate function in terms of reliability. Reliab. Eng. Syst. Safe. 75, 397–406.